Article

Photoprintable Gelatin-*graft*-Poly(trimethylene carbonate) by Stereolithography for Tissue Engineering Applications

Thomas Brossier, Gael Volpi, Jonaz Vasquez-Villegas, Noémie Petitjean, Olivier Guillaume,
Vincent Lapinte, and Sébastien Blanquer*

Cite This: https://doi.org/10.1021/acs.biomac.1c00687

Read Online

ACCESS | Metrics & More | Article Recommendations | Supporting Information

ABSTRACT: The stereolithography process is a powerful additive manufacturing technology to fabricate scaffolds for regenerative medicine. Nevertheless, the quest for versatile inks allowing one to produce scaffolds with controlled properties is still unsatisfied. In this original article, we tackle this bottleneck by synthesizing a panel of photoprocessable hybrid copolymers composed of gelatin-*graft*-poly(trimethylene carbonate)s (Gel-*g*-PTMC$_n$). We demonstrated that by changing the length of PTMC blocks grafted from gelatin, it is possible to tailor the final properties of the photofabricated objects. We reported here on the synthesis of Gel-*g*-PTMC$_n$ with various lengths of PTMC blocks grafted from gelatin using hydroxy and amino side groups of the constitutive amino acids. Then, the characterization of the resulting hybrid copolymers was fully investigated by quantitative NMR spectroscopy before rendering them photosensitive by methacrylation of the PTMC terminal groups. Homogeneous composition of the photocrosslinked hybrid polymers was demonstrated by EDX spectroscopy and electronic microscopy. To unravel the individual contribution of the PTMC moiety on the hybrid copolymer behavior, water absorption, contact angle measurements, and degradation studies were undertaken. Interestingly, the photocrosslinked materials immersed in water were examined using tensile experiments and displayed a large panel of behavior from hydrogel to elastomer-like depending on the PTMC/gel ratio. Moreover, the absence of cytotoxicity was conducted following the ISO 10993 assay. As a proof of concept, 3D porous objects were successfully fabricated using stereolithography. Those results validate the great potential of this panel of inks for tissue engineering and regenerative medicine.
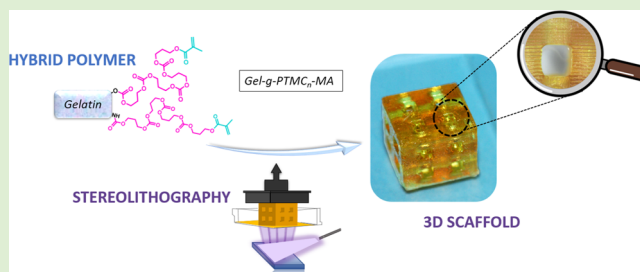
1. INTRODUCTION

Tissue engineering (TE) is one of the most promising approaches for the biomedicine of tomorrow. Most of the TE strategies rely on the use of biomaterials and on their processing to create temporary scaffolding structures. However, despite significant efforts, proposing a universal strategy that could generate an ideal scaffold for tissue engineering remains a considerable challenge. Indeed, such scaffolds must not only be biocompatible, biodegradable, and porous but must also display sufficient mechanical properties and be endowed with biofunctionalities such as promoting cellular adhesion and proliferation.[1] In that sense, one of the crucial steps in the TE strategy is the choice of the polymer material.

In this context, a broad variety of natural biopolymers and synthetic polymers has been integrated in the composition of the TE scaffold.[2,3] More particularly, synthetic-based polymers with specific biodegradability and tunable properties have been extensively used for scaffold production.[4,5] Among them, the family of aliphatic polycarbonates, with the gold standard being poly(trimethylene carbonate) (PTMC), has been largely assessed as a scaffold for bone,[6] cartilage[7] or intervertebral disc tissue.[8] PTMC is especially recognized (i) for its specific

biodegradation by surface erosion, which then does not compromise the mechanical properties during the degradation process, and (ii) for its elastomer-like property, especially upon curing.[9] Moreover, the typical carbonate functions lead to the absence of acidic by-products generated upon degradation, which has been recognized as a huge advantage in tissue reconstruction.[10] However, despite such promising interest, PTMC remains highly hydrophobic with no cell recognition sites, which explains the difficulty for the cells to adhere onto it.[11] To overcome those limitations, an attractive approach is to combine such synthetic-based materials with biopolymers originating from the extracellular matrix.[12,13]

Biopolymers are widely recognized to be an effective matrix for TE scaffolds especially because of their remarkable affinity with water and similarity with the native tissue composition.
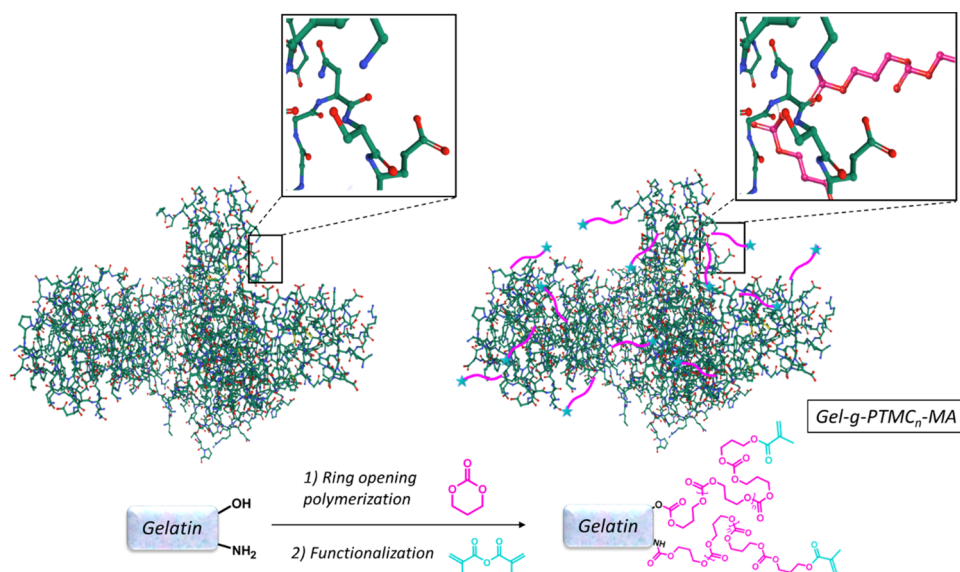
Figure 1. Schematic molecular overview and chemical pathway of the PTMC (pink) grafted from the gelatin and functionalized for further photofabrication (blue) (Gel-*g*-PTMC*n*-MA).

However, those biopolymers display often weak mechanical properties and their degradation kinetics remains inappropriate to be used as a single component of any scaffolds.[14] Hence, the approach could consist in developing a hybrid polymer based on PTMC to confer suitable mechanical performances and extracellular matrix biopolymers to endow the biomaterials with effective bioactivity. Several biopolymers from the extracellular matrix have been already investigated in the reconstructive tissue area including collagen, gelatin, fibrin, elastin, and glycosaminoglycan.[15,16] Gelatin remains one of the most traditional natural polymers in TE.[17,18] Gelatin is a protein derived from the denaturation of collagen, which then allows one to provide favorable cellular bioadhesion due to the numerous RGD sequences. Multiple chemical strategies have been attempted to improve its mechanical properties either by grafting poly(ethylene glycol) (PEG) onto the gelatin,[19,20] by crosslinking it *via* enzymes,[21] or by photopolymerization of methacryloyl gelatin (Gel-MA).[22] Nevertheless, those processes have still limited successes and the achieved mechanical strengths are still far from being suitable.

Consequently, the synthesis of a hybrid material based on gelatin and PTMC that will not only reinforce the mechanical properties of the gelatin but also significantly improve the cell response of the raw PTMC would be of great interest. However, the synthesis of such hybrid materials is challenging, mainly because of the physical and chemical incompatibility between the hydrophobic nature of PTMC and the highly hydrophilic natural biopolymers. Hence, the reported blend approach requires specific conditions to yield a homogeneous phase and, most of the time, involved the use of a toxic or hazardous solvent.[23] An alternative of the blend approach has been recently reported by Grijpma *et al.*, which consists in a hybrid network of Gelatin-PTMC obtained from blended methacrylated macromonomer precursors and subsequently photocured.[24] Despite promising mechanical properties, homogeneous dispersion can only be reached by using a harsh solvent with a high level of dilution, which then limits the possibility to use such a system for scaffold fabrication by additive manufacturing. Unlikely, from another perspective, PTMC has been coupled as a hybrid block terpolymer with

other type of extracellular matrix such as elastin[25] and hyaluronic acid[26] to generate amphiphilic and self-assembled block copolymers. But, to the best of our knowledge, directly grafting PTMC on gelatin is an approach never reported so far in the literature.

We propose here hybrid copolymers, gelatin-*graft*-poly-(trimethylene carbonate)s (Gel-*g*-PTMC*n*), obtained by the "grafting-from" approach using TMC monomers and specific reactive functions of the gelatin as a macroinitiator (Figure 1). In designing and synthesizing such complex materials, the lack of chemical characterizations remains a recurrent issue, which is required to elucidate the individual role of each component on the final behavior of the copolymer structure. Therefore, efforts have been devoted in this work to fully characterize the hybrid material using several lengths of PTMC block grafted from the gelatin. We further functionalized the Gel-*g*-PTMC*n* copolymers by inserting photosensitive functions to generate a photocrosslinked network. We then tested the photocrosslinked hybrid copolymers in terms of mechanical properties, cytocompatibility, and degradability. Finally, the photosensitive Gel-*g*-PTMC*n* copolymers were also used to validate their processability by 3D printing technology using vat photopolymerization such as stereolithography (SLA). SLA is recognized for its remarkable efficiency and considerable advantages in terms of versatility in manufacturing, high accuracy, and speed.[27] In consequence, we proposed here an attractive option, as it is a versatile and controlled approach, allowing one to generate a large variety of hybrid materials based on gelatin and PTMC without any issue of miscibility and which can be used to fabricate 3D porous scaffolds using SLA.

2. EXPERIMENTAL SECTION

2.1. Materials. Trimethylene carbonate (TMC) was provided by Foryou Medical Devices, China. Gelatin from porcine skin (type A, gel strength 300 g Bloom), triethylamine (TEA), methacrylic anhydride, hexamethyldisilazane, anhydrous dimethyl sulfoxide (DMSO), dichloromethane (DCM), phosphate-buffered saline (PBS), 1,5,7-triazabicyclo[4.4.0]dec-5-ene (TBD), stannous octanoate, and hexamethyldisilazane were purchased from Sigma-Aldrich,

France. Darocur 1173 was acquired from BASF (Germany). Orange G dye comes from TCI, Japan. The reagents and solvents were of analytical grade and were used as received.

2.2. Synthesis and Formulation. *2.2.1. Synthesis of Gelatin Methacrylate (Gel-MA).* Gel-MA was synthesized according to the previously published method.[28] Briefly, 10 g of porcine gelatin type A (0.015 mol, 1 equiv) was dissolved in 200 mL of PBS under continuous stirring at 50 °C. Then, methacrylic anhydride (0.06 mol, 4 equiv) and triethylamine (0.06 mol, 4 equiv) were added dropwise to the solution. The reaction was stirred vigorously at 50 °C for 2 h. The solution was then dialyzed against deionized water using a dialysis tubing (cutoff: 8 kDa) at 50 °C for 1 week to remove salts and unreacted methacrylic anhydride. The Gel-MA solution was freeze-dried, resulting in porous Gel-MA foam stored until use.

2.2.2. Synthesis of PTMC by Ring-Opening Polymerization. The synthesis of 50 g of PTMC (M_n = 10,000 g/mol) was carried out by ring-opening polymerization of TMC (0.49 mol, 100 equiv), initiated by 1,6-hexanediol (0.0049 mol, 1 equiv), and catalyzed by stannous octanoate at 130 °C (0.05 wt %) for 24 h under inert N_2 gas. After cooling to room temperature, PTMC was dissolved in dried dichloromethane (50 mL) and precipitated in cold methanol. The precipitate was filtered and dried in the dark under ambient conditions overnight.

2.2.3. Synthesis of Grafted PTMC from the Gelatin (Gel-g-PTMC$_n$). Gel-g-PTMC$_n$ (n = 6, 10, 16, and 32) were obtained *via* ring-opening polymerization in solution. Briefly, for the synthesis of Gel-g-PTMC$_6$, 1 g of gelatin (on the basis of the known composition, the amounts of available amine groups and hydroxyl groups for 1 g of gelatin represent 0.29 and 1.5 mmol, respectively[29]) was charged in a round-bottom flask under an inert nitrogen atmosphere and dissolved in dry DMSO (20 mL). The solution was stirred at 50 °C until full gelatin dissolution before the addition of TMC (10 mmol, 5 equiv regarding the amount of active groups from the gelatin) monomer. The proportion of TMC is adjusted regarding the expected *n* ratio of PTMC. The mixture was stirred at 50 °C until complete consumption of the free amino pendant groups as described in our previous report,[30] followed by the addition of the TBD catalyst (0.9 mmol, 0.5 equiv regarding the amount of active groups from the gelatin). The polymerization reaction was stirred at 50 °C under an inert nitrogen atmosphere and the conversion was followed by ^{1}H NMR spectroscopy. After the reaction was completed, the crude was precipitated into water and washed with ethanol. Exception was done for the determination of ROP initiation where the reaction was stopped just after the beginning of the polymerization, then purified by dialysis, and analyzed by ^{1}H NMR spectroscopy in D_2O.

2.2.4. Synthesis of PTMC and Methacrylated Gel-g-PTMC$_n$ (Gel-g-PTMC$_n$-MA). PTMC and Gel-g-PTMC$_n$ were end-functionalized with methacrylate groups using methacrylic anhydride (4 equiv) in the presence of triethylamine (4 equiv) in dichloromethane (50 wt %). For all the formulations, the solution was then stirred in the dark for 3 days at room temperature under a nitrogen atmosphere. The mixtures were precipitated in cold ethanol, and the precipitates were filtered and dried in the dark under ambient conditions overnight. The final products were stored at 4 °C until further use.

2.3. Characterization and Measurements. *2.3.1. Nuclear Magnetic Resonance Spectrometry.* ^{1}H NMR, DOSY NMR, and quantitative ^{13}C NMR spectra were recorded on 400 and 500 MHz Bruker Aspect spectrometers. $CDCl_3$ and D_2O were used as deuterated solvents. Chemical shifts were given in parts per million (ppm). The reference peaks were residual D_2O at 4.79 ppm for ^{1}H NMR or $CDCl_3$ at 7.26 and 77 ppm for ^{13}C NMR. Conversion was also determined by ^{1}H NMR spectroscopy. The degree of polymerization (DP$_n$) was calculated from quantitative ^{13}C NMR according to eq 1.

$$\mathrm{DP}_n = \frac{\int c_{62\mathrm{ppm}}/2}{\int c_{59\mathrm{ppm}}} \tag{1}$$

2.3.2. Complex Viscosity. Gel-g-PTMC$_n$ polymers were diluted in 20 wt % DMSO. The viscosity properties were investigated by

performing complex viscosity measurements. Viscoelastic properties of Gel-g-PTMC$_n$ solutions were measured using a rheometer apparatus (Physica Modular Compact MCR301, Anton Paar, Germany) at frequencies ranging from 0.1 to 10 Hz (0.6 to 62.8 rad s^{-1}) at 25 °C. Oscillatory shear measurements were conducted using a 40 mm 2° diameter steel cone with a truncation gap of 55 μm to measure the complex viscosity (η^*) and deduce the zero-shear viscosity (η_0) at 0.1% strain.

2.3.3. Crosslinker Chamber and Building. Films were photo-crosslinked in a UV Crosslinker Biolink chamber (Thermo Fisher, France) using UV lamps with a broad wavelength (maximum peak at 365 nm). Irradiation was performed at room temperature at 10 cm from the surface of the specimens, and the intensity was around 2−3 mW/cm^2 for 10 min.

2.3.4. Degree of Swelling. The swelling behavior and water uptake properties of the Gel-g-PTMC$_n$ networks were performed on photocrosslinked disk films (1 cm in diameter and 2 mm in thickness). Samples were initially dried after irradiation and then weighted to obtain the initial mass (m_i). Then, samples were incubated in distilled water for 24 h (water was renewed five times). After swelling, the polymers were weighed to determine the swollen mass (m_s) and vacuum-dried to determine the dry mass (m_d).

The photocrosslinking efficiency was calculated by the gel content (eq 2) and the water absorption was determined by the equilibrium water content (EWC) (eq 3).

$$\mathrm{gel\ content} = \frac{m_d}{m_i} \times 100 \tag{2}$$

$$\mathrm{EWC} = \frac{m_s - m_d}{m_s} \times 100 \tag{3}$$

2.3.5. Contact Angle. Disk samples (1 cm in diameter and 2 mm in thickness) of the photocrosslinked Gel-g-PTMC$_n$ were initially prepared and the measures were performed on extracted (three times in DCM) and dried samples. Contact angle measurement (G10 optical, Krüss, Germany) was conducted to determine the surface tension by depositing water drops on three different areas of the films with a microsyringe.

2.3.6. Scanning Electronic Microscopy and Energy-Dispersive X-ray Spectroscopy. The surface elemental compositions of photo-crosslinked Gel-g-PTMC$_n$ films were determined on extracted and dried samples (1 cm in diameter and 2 mm in thickness). The analyses were performed using scanning electronic microscopy (SEM) (Phenom-World ProX) coupled with energy-dispersive X-ray spectroscopy (EDX) using an accelerating voltage of 15 kV. Prior to SEM analysis, samples were freeze-dried and sputter-coated with gold. Mapping quantification analysis was performed using the dedicated Thermo Scientific Phenom Elemental Mapping Software. Results are given in % of atomic element.

2.3.7. Mechanical Measurements. The dumbbell shape (ISO527-2) of the Gel-g-PTMC$_n$ network was first molded, and the samples were then extracted and dried under vacuum at room temperature for one night. The films were then immersed in water for 24 h. The samples were immersed in water, and the elongation at break and Young modulus were measured with an Instron3366L5885 tensile tester. The cross-head speed was 5 mm·s^{-1}. The elongation at break was expressed as a percentage of the original length and the modulus was obtained at 0.5% deformation by stress/strain.

2.3.8. Evaluation of Cytotoxicity of the Crosslinked Polymers. The cytocompatibility of the different Gel-g-PTMC$_n$ networks (with increasing percentage of PTMC, from DP$_6$ to DP$_{32}$) was tested *via* extraction tests in accordance with the ISO 10993-5 guidelines to detect the presence of cytotoxic compounds released from the samples into the media.

The extract test was conducted by immersing crosslinked copolymer disks (surface area: 1.25 cm^2 mL^{-1}) in an extraction vehicle, consisting of cell culture medium, i.e., high-glucose Dulbecco's modified Eagle medium (HG-DMEM, Gibco, United Kingdom) supplemented with 10% newborn calf serum (NCBS) and 1% penicillin−streptomycin. This incubation was conducted at 37 °C
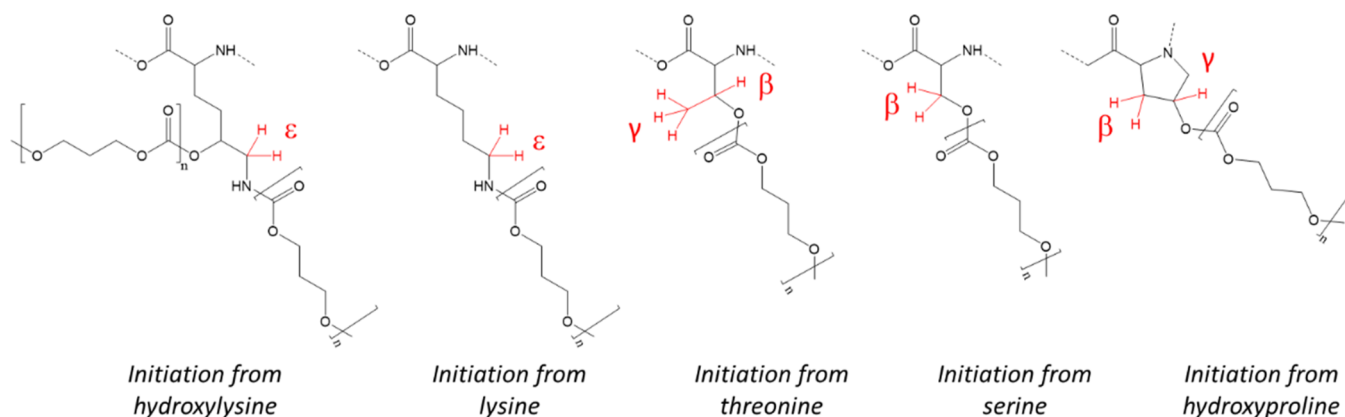
Figure 2. Resulting chemical structure after the ROP of TMC from amino acids of the gelatin.

for 3 days. Next, the extracts were collected and used as feeding media for L929 fibroblasts.

The L929 fibroblasts were seeded at a density of 5.0×10^3 cells well^{-1} in 96-well plates and cultivated until reaching approximately 70% confluency. Next, the culture medium was removed and the cells were incubated in 100 μL of the extracts for 24 h ($n = 6$). Extract-free HG-DMEM was applied as the feeding medium for the cells as the positive control, whereas a culture medium supplemented with 5% DMSO was applied as the feeding medium for the cells as the negative control.

The metabolic activity of the L929 fibroblasts was assessed using PrestoBlue Cell Viability Reagent (Invitrogen, Fisher Scientific, Vienna, Austria) at 24 h of the culture. The fluorescence of the medium was recorded ($\lambda_{ex} = 560$ nm; $\lambda_{em} = 590$ nm) using a plate reader (Synergy H1 BioTeK plate reader, Bad Friedrichshall, Germany). The fluorescence value obtained for the cells cultivated in the extract-free medium was considered as 100% viability for each time point. The fluorescence values of the sample extracts were normalized against the corresponding control group and expressed relative to this 100% viability. The morphology of the cells spreading onto the plastic of 96-well plates was observed by taking images after the extract test using bright-field imaging of the LSM700 (Zeiss, Germany), mag. 20 (Camera AxioCam 105).

The morphology of the cells spreading directly onto the surface of Gel-g-PTMC$_n$ was observed by seeding 10.0×10^3 cells of L929 fibroblasts onto the film (2 mm in thickness and 10 mm in diameter). After 3 days of incubation in HG-DMEM supplemented with 10% NCBS and 1% penicillin–streptomycin, the samples were retrieved for scanning electron microscopy observation (SEM Philips XL Series 30). Briefly, samples were washed in PBS and fixed in buffered paraformaldehyde at 4%, followed by gradual dehydration in ethanol and by immersion in hexamethyldisilazane. After drying, the samples were sputter-coated with Au and investigated by SEM.

2.3.9. Degradation Study. In vitro degradation of the Gel-g-PTMC$_n$ networks (1 cm in diameter and 2 mm in thickness) was evaluated in harsh conditions to accelerate the degradation process. Dried samples were placed in NaOH solution (1 M) at 40 °C. Before and after incubation (4, 6, and 8 h), specimens were collected, wiped, and deposited on a glass plate to visualize the degradation.

2.3.10. 3D Structures with Stereolithography Apparatus. To prepare resin formulations for SLA processing, Gel-g-PTMC$_n$ were mixed with DMSO (40 wt %) as nonreactive diluents. Darocur 1173 (3 wt % relative to the polymer) and Orange G (0.2 wt % relative to polymer) were added as a photoinitiator and dye agent, respectively.

Cubic three-dimensional porous structures with an average pore size and strut of 1 mm were designed using the STL format from Rhinoceros 3D. The 3D structures were built from the above-mentioned resins by stereolithography (SLA) using a digital light processing (DLP) apparatus (Asiga Max X27, Australia). The 3D objects were constructed in the DLP apparatus by photocrosslinking subsequent layers of resin with thicknesses of 100 μm, upon which a

pixel pattern was projected. Each layer was illuminated at an intensity of 20 mW/cm^2 for 30 s. After building, the structures were washed with DMSO and extracted for 72 h with DCM to leach out DMSO. The final structures were dried after 2 days at room temperature.

3. RESULTS AND DISCUSSION

3.1. Grafting-from Strategy. By definition, the term of covalent grafting on polymers is applied to define one of the three following grafting methods: "grafting-to", "grafting-through", and "grafting-from". In this work, we proposed to focus on the "grafting-from" method where the graft copolymers grow *in situ* from the active functions of the initial backbone polymer. In comparison to other methods, hybrid polymers obtained by the grafting-from approach lead to highly ramified grafted copolymers because of the polymer–monomer reaction, which is less affected by steric hindrance than the other polymer–polymer reactions. Moreover, the purification steps are remarkably simpler as the separation of the resultant grafted copolymers from unreacted monomer precursors can be easily done by precipitation. However, the grafting-from method remains rarely employed especially because of the difficulty to characterize the ratio of the grafted copolymer. Such observation is even more true in the case of amphiphilic copolymers, especially due to the incompatibility between the blocks, which renders the characterization complex. We therefore particularly focused this work on the characterization procedure to prove the efficiency of the grafting and to determine the proportion of TMC grafted from the gelatin.

PTMC grafting from the gelatin has been done by ring-opening polymerization (ROP) of the monomer TMC from the specific active functions on the gelatin susceptible to initiate ROP. All amino acids exhibit a pendant alcohol function, which can actually be involved in the initiation of ROP. Moreover, we recently demonstrated that amino groups were also able to initiate the ROP of TMC, which then generates urethane functions.[30] Therefore, the amino acids susceptible to initiate the ROP of TMC from the gelatin might be serine (0.328 mmol/g), threonine (0.144 mmol/g), hydroxyproline (0.902 mmol/g), lysine (0.259 mmol/g), and hydroxylysine (0.066 mmol/g)[31−33] (Figure 2).

To avoid the presence of residual metal in the final material, we decided to ban metallocatalysts and oriented the study toward organocatalysts, in particular nucleophilic catalysts such as TBD. To prevent any gelatin degradation, the TBD reaction was conducted at low temperatures.[34] The ROP of TMC using

the TBD catalyst has already been investigated with alcohol[35,36] or amine group initiation,[30] even though the latter one requires multiple steps. Indeed, a previous work demonstrated that the ROP with TBD initiation by amine groups must be done in two successive steps, the first being the ring opening of one TMC unit in the absence of a catalyst followed by classic ROP initiated by the generated hydroxy groups.[37] Therefore, the ROP initiation of TMC was activated from the alcohol and amine functions of the gelatin. Finally, it is also crucial to not neglect the type of solvent that will be used, as it must be able to solubilize the gelatin, the TMC monomers, and the resulting hybrid polymer. DMSO was selected to perform the ROP of TMC as this solvent fulfills this requirement, and further, it is recognized as being a low hazardous solvent, in contrast to the traditional solvent used for the synthesis of hybrid copolymers.

Several ratios of PTMC have been synthesized, and the reaction yields reached in average 92 ± 4% for all the hybrid polymers, which then indicates the high performance of the reaction. It can be noticed that the physicochemical behavior of the resulting materials, especially the solubility, differs from the proportion of PTMC, which will then result in a serious issue for the characterization. Therefore, to get a global and correct characterization of the grafting, a diagonal approach was undertaken using first ^{1}H NMR in D_2O to validate the ROP initiation from the gelatin, while quantitative ^{13}C NMR spectroscopy in $CDCl_3$ was used to determine the proportion of grafted PTMC.

3.1.1. Validation of ROP Initiation from Gelatin Using ^{1}H NMR in D_2O. ^{1}H NMR spectroscopy in D_2O has been used to determine the initiation process of TMC from the gelatin. Indeed, D_2O was the most appropriate solvent to characterize the gelatin with well-defined and attributed characteristic protons of amino acids, especially those involved in the ROP initiation (Figure 3). Therefore, to keep the solubility in water, the analyses in D_2O must be performed at the beginning of the polymerization, just at the initiation of TMC by the active functions of the gelatin.

From the ^{1}H NMR spectrum of the gelatin, the characteristic peaks of the amino acids involved in the ROP initiation (serine, threonine, lysine, hydroxylysine, and hydroxyproline) were assigned (Figure 3 and Table 1). Upon polymerization of the TMC monomers, the characteristic peaks from such amino acids shifted, which proved the grafting (Figure 3A and Table 1). Based on the study from Claassen *et al.* on methacryloyl gelatin,[31] it has been possible to assign each shifted peak attributed to the modified amino acids once the polymerization was initiated. Such peak shifting can be also correlated with the growing signal of the characteristic peaks from the PTMC polymer at 2 and 4.2 ppm. Moreover, to ensure the grafting of PTMC on the gelatin, a DOSY NMR analysis in D_2O was performed. In Figure 3B, the single diffusion coefficient demonstrated the presence of both gelatin and PTMC within the same macromolecule, and consequently, it proves the successful grafting-from approach for the synthesis of hybrid polymers. However, it must be noticed that in return, quantitative ^{13}C NMR spectroscopy of grafted gelatin in D_2O is not sufficiently consistent because of the high complexity of the spectra, and the determination of the grafted PTMC ratio cannot be identified as long as the hybrid copolymer remains soluble in water.

3.1.2. Quantification of Grafted PTMC by Quantitative ^{13}C NMR Spectroscopy in $CDCl_3$. Even though the
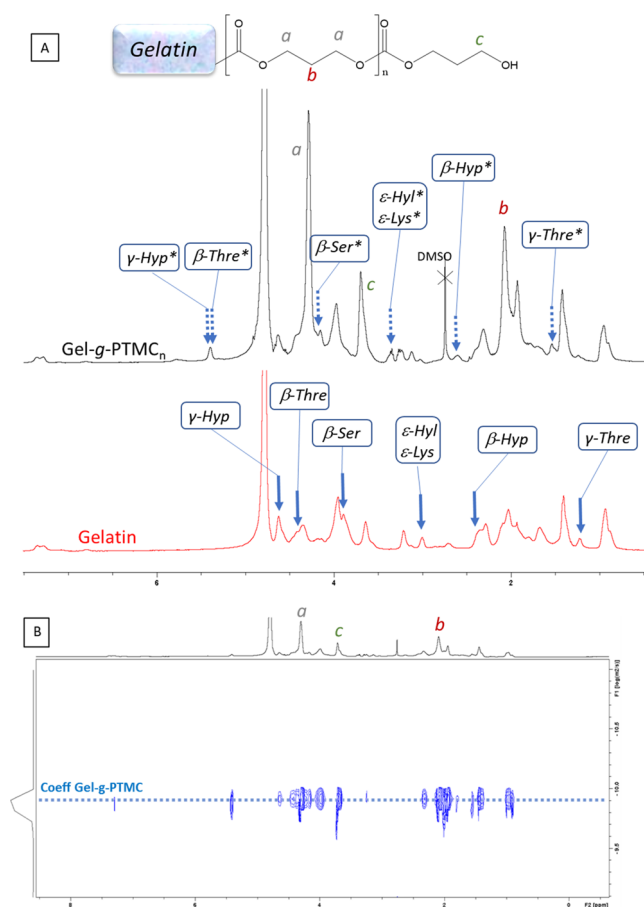
Figure 3. D_2O ^{1}H NMR spectra of native gelatin and Gel-*g*-PTMC$_n$ (A), with full line arrows to show the characteristic peaks of the amino acids involved in the ROP from the gelatin and dotted line arrows and asterisks for the modified amino acids from Gel-*g*-PTMC$_n$ (Table 1); D_2O DOSY NMR spectrum of Gel-*g*-PTMC$_n$ (B).

Table 1. Chemical Shift of Characteristic Peaks from the Amino Acids Involved in ROP Initiation

characteristic proton of the amino acids involved in ROP initiation	amino acid abbreviation	chemical shift of protons before ROP (ppm)	chemical shift of protons after ROP (ppm)
γ-threonine (CH$_3$)	γ-Thr	1.2	1.5
β-threonine (CH)	β-Thr	4.3	5.4
β-serine (CH$_2$)	β-Ser	3.9	4.1
ε-hydroxylysine (CH$_2$)	ε-Hyl	3.0	3.3
ε-lysine (CH$_2$)	ε-Lys	3.0	3.3
γ-hydroxyproline (CH)	γ-Hyp	4.6	5.5
β-hydroxyproline (CH$_2$)	β-Hyp	2.4	2.6

quantification in D_2O was not possible, ROP initiation from the gelatin was successfully demonstrated. Therefore, it was relevant for us to reach higher ratios of PTMC to finally be potentially able to quantify the grafting. However, the threshold of solubility of the hybrid copolymer from water to the organic solvent is narrow, and the Gel-*g*-PTMC$_n$ becomes rapidly insoluble in water once PTMC chains are growing. Consequently, as the gelatin fraction is not soluble in an organic solvent, only the PTMC blocks from the copolymer were visualized by NMR spectroscopy in $CDCl_3$. We investigated the possibility of quantitative ^{13}C NMR spectroscopy to measure the average size of grafted PTMC from the gelatin. As shown in Figure 4A, the end-chains were easily
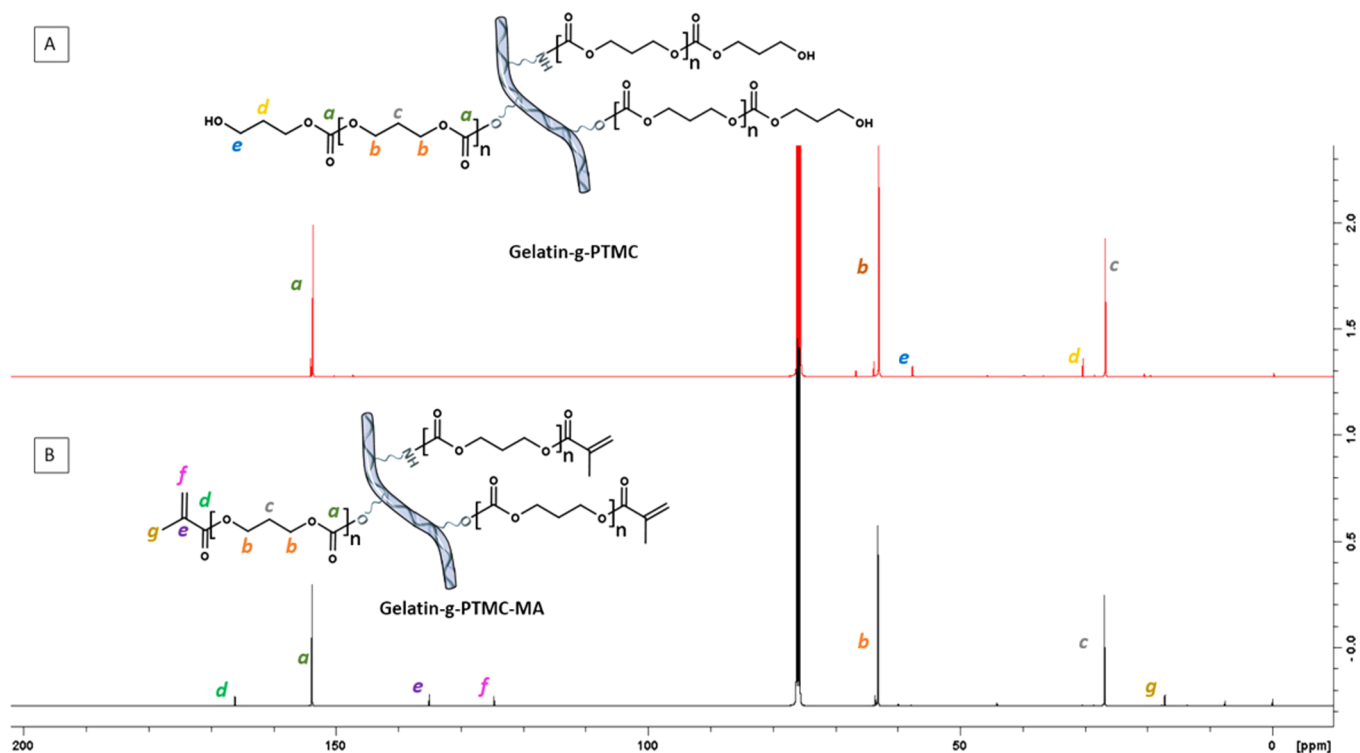
Figure 4. Quantitative ^{13}C NMR spectrum of Gel-g-PTMC$_n$ (A) and, after methacrylation, Gel-g-PTMC$_n$-MA (B) in CDCl$_3$.

Table 2. Mechanical Properties of Hydrated Photocrosslinked Gelatin, PTMC, and Gel-g-PTMC$_n$

	σ_{max} (MPa)	ε_{max} (%)	Young modulus (MPa)	gel content[a] (%)	water uptake[b] (%)
gelatin	0.16 ± 0.03	18.63 ± 3.96	0.74 ± 0.13	70.9 ± 0.5	71.2 ± 0.4
Gel-g-PTMC$_6$	0.52 ± 0.18	13.73 ± 3.75	4.62 ± 0.84	81.9 ± 0.6	8.7 ± 0.7
Gel-g-PTMC$_{10}$	1.07 ± 0.14	52.96 ± 8.12	2.76 ± 0.20	89.6 ± 1.4	3.8 ± 1.1
Gel-g-PTMC$_{16}$	1.19 ± 0.04	59.58 ± 0.46	2.43 ± 0.05	90.9 ± 0.8	2.4 ± 0.5
Gel-g-PTMC$_{32}$	0.48 ± 0.06	96.39 ± 16.10	0.95 ± 0.09	97.3 ± 2.2	2.2 ± 0.4
PTMC	1.53 ± 0.29	327.30 ± 6.89	1.29 ± 0.17	95.9 ± 1.1	1.3 ± 0.2

[a]Determined with the equation and performed in DMSO (eq 2). [b]Determined with eq 3.

distinguishable at 59 ppm, while the peak at 62 ppm represents the aliphatic carbons of the PTMC chain and, at 154 ppm, the carbon of the carbonate functions. By comparing the peak intensity using eq 1, the number of TMC grafted from the gelatin can be calculated and the average chain size of PTMC can be subsequently deduced. As schematized in Figure 1, gelatin is a huge protein compared to the PTMC chains, and therefore, we chose a nomenclature that takes into consideration the different ratios of PTMC regarding their DP$_n$ rather than the ratio of PTMC related to gelatin. We determined four different grafting ratios named as Gel-g-PTMC$_6$, Gel-g-PTMC$_{10}$, Gel-g-PTMC$_{16}$, and Gel-g-PTMC$_{32}$. It is crucial to mention that the conversion rates measured by ^{1}H NMR spectroscopy were around 93 ± 2% for all the synthesized Gel-g-PTMC$_n$. Consequently, the high degree of conversion with satisfying yield of reaction coupled with DOSY NMR spectroscopy can ensure that all TMCs were grafted on the gelatin.

Finally, the last step to obtain photosensitive polymers for SLA fabrication consists in the functionalization of the hybrid polymers by methacrylate active moieties. This approach is now widely used and recognized to be efficient to lead to photocrosslinkable polymers.[38] The functionalization was followed by quantitative ^{13}C NMR spectrometry with the

apparition of the characteristic signal of the carbonyl from the grafted methacrylate at 168 ppm (Figure 4B). The proportion of the methacrylate group was calculated by comparing the characteristic peaks of the methacrylate carbonyl with those of the carbonyl from the PTMC chains at 152 ppm. For all the hybrid polymers, we reached an average of 80 ± 3% of grafted methacrylate functions.

The rheological viscosity measurement in DMSO was monitored on Gel-g-PTMC$_n$ samples to determine the influence of the length of PTMC blocks grafted on a gelatin backbone. This characterization is essential for our application, as it is well known that viscosity is a leading parameter for further stereolithography processing. As shown in Figure S1, the Gel-g-PTMC$_n$ viscosity was not dependent on the frequency in contrast to the native gelatin. The grafting of PTMC on the gelatin biomacromolecule stabilized the rheological behavior in frequency as pristine PTMC. Moreover, the higher the DP$_n$ of PTMC is, the higher the viscosity is, ranging from 0.24 to 136.7 MPa·s for DP$_6$ and DP$_{32}$, respectively. The viscosity depended highly on the ramifications of the macromolecular structure, and consequently, an exponential enhancement of the viscosity can be noted, which corroborates the proportion of PTMC calculated by NMR.

The presence of longer PTMC chains increases the chain entanglement, which then amplifies the viscosity of the resin.

3.2. Physical Properties of Photocrosslinked Hybrid Copolymers Gel-*g*-PTMC$_n$. The photosensitive hybrid polymers Gel-*g*-PTMC$_n$-MA in 20 wt % DMSO were then successfully photocrosslinked in a UV crosslinker chamber at 365 nm after 10 min in the presence of a photoinitiator Darocur 1173 at room temperature. The complete consumption of the photoreactive methacrylate units has been checked by FT-IR spectroscopy regarding the characteristic C=C band at 1640 cm^{-1} (data not shown). The network materials were characterized by various techniques to demonstrate the impact of PTMC on gelatin on both the surface and the inner part of films from the resulting materials.

First of all, the photocrosslinking density was determined by the measurement of gel content (Table 2). It appears that for the grafted PTMC above DP$_{10}$, the networks were formed with a gel content between 81 and 95% in DMSO. As previously established, DMSO was the best solvent to solubilize the gelatin and TMC monomers. DMSO was consequently used for copolymer photocrosslinking and for investigating the gel content. However, the gel content for photocrosslinked gelatin and Gel-*g*-PTMC$_6$ was found not to be optimal in this solvent compared to PTMC or copolymers of higher DP. This behavior can be due to a lower solubility of gelatin and Gel-*g*-PTMC$_6$ in DMSO, which then reduces slightly the efficacy of the photocrosslinking reaction.

The only moiety of the hybrid Gel-*g*-PTMC$_n$ bearing nitrogen atoms is the gelatin. Consequently, the percentage of nitrogen can be an efficient probe to estimate the amount of gelatin in the Gel-*g*-PTMC$_n$ network. The SEM images were undertaken on the Gel-*g*-PTMC$_n$ film after cross section to get access to the inner part of the materials (Figure S2), and no observation of phase separation could be visualized. The chemical homogeneity of the samples was then determined by the SEM−EDX analysis (Figure 5A) for nitrogen investigation. First, as shown in the mapping quantification, similar amounts of nitrogen were detected in different points of each Gel-*g*-PTMC$_n$ network film, demonstrating the homogeneous distribution of the gelatin for each hybrid copolymer without phase segregation. Second, as expected, the proportion of nitrogen decreased when the length of PTMC blocks in the Gel-*g*-PTMC$_n$ network increased, as shown in Figure 5A. Interestingly, such evolution is proportionately following the same trend as the DP$_n$ of the grafted PTMC.

The Gel-*g*-PTMC$_n$ network composition also influenced the hydrophilic behavior of the films, as illustrated by contact angle measurement (Figure 5B). We noted a round drop on the surface of pristine photocrosslinked PTMC and Gel-*g*-PTMC$_n$ with PTMC chains above DP$_{10}$. The values were close to 100°, a typical value of a hydrophobic surface. By contrast, for pure gelatin or the Gel-*g*-PTMC$_6$ network, the contact angle decreased to 55−65° with a spread drop on the surfaces. The regular increase in contact angle value with the length of the PTMC blocks demonstrates the hydrophobization of the surface along with the PTMC content.

The hydrophilic behavior of such hybrid polymers is crucial to foresee any tissue engineering applications. Hence, in correlation with the contact angle measurements, the capacity of the Gel-*g*-PTMC$_n$ networks to absorb water was determined by the water uptake study (Table 2). The Gel-*g*-PTMC$_n$ adsorption values were gathered into the region from 2.2% to 8.7%. As expected, the most hydrophilic materials, owing to
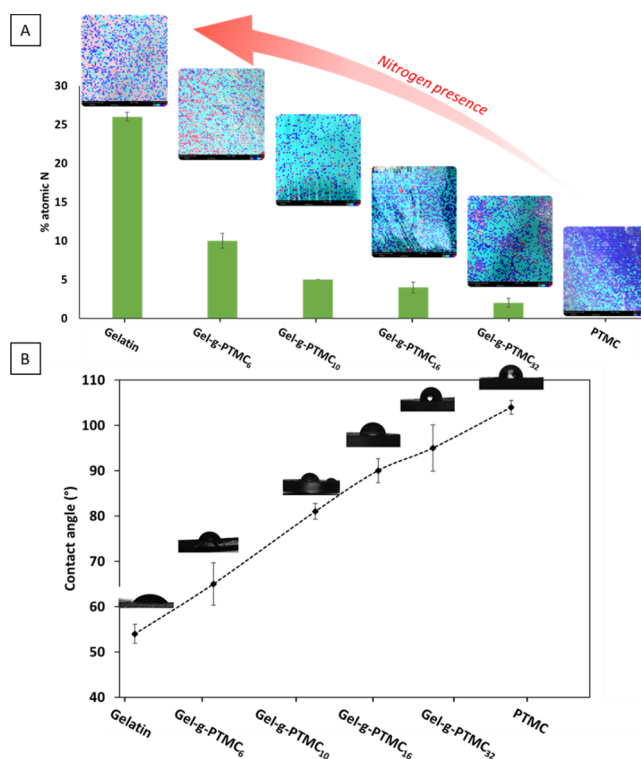
Figure 5. Nitrogen amount of photocrosslinked film's cross sections analyzed by SEM−EDX (red for nitrogen, blue for oxygen, and green for carbon) (A) and contact angle on the Gel-*g*-PTMC$_n$ surface (B).

the highest water uptake values, were the pure photocrosslinked gelatin and the Gel-*g*-PTMC$_n$ bearing the shortest PTMC chains. In contrast, pure photocrosslinked PTMC and Gel-*g*-PTMC$_n$ bearing the longest PTMC chains exhibited more hydrophobic properties. Despite a non-neglected water uptake, the samples do not swell in water, which can be considered as a favorable parameter for our targeted application. Indeed, materials that do not swell in water have reduced risks of deformation and more stable mechanical properties.

3.3. Mechanical Properties of the Hybrid Material Gel-*g*-PTMC$_n$ Network. The tensile test experiments conducted under water immersion were realized on the photocrosslinked PTMC and gelatin samples as well as on Gel-*g*-PTMC$_n$ networks (Figure 6 and Table 2). As reported in the literature, the singular behavior of crosslinked gelatin (low elongation at break, 18%; maximum stress, 0.16 MPa)[39] contrasted with crosslinked PTMC (higher elongation at break, 327%; maximum strain, 1.53 MPa).[40,41] Our results corroborated such findings. For the Gel-*g*-PTMC$_n$ network, the values ranged in a region between the properties of the gelatin and PTMC. From the resulting data, the evolution of the properties that are following three distinct trends can then be identified.

First of all, already for the Gel-*g*-PTMC$_6$ network, the mechanical properties are substantially improved compared to photocured gelatin in terms of maximum stress and elastic modulus. Then, by increasing the degree of polymerization of grafted PTMC, the Young modulus starts to significantly decrease, while the maximum stress and strain increase. Hence, 13% elongation at break was measured for short PTMC chains, whereas 96% was reached for DP$_{32}$ of PTMC (Table 2). Finally, the Gel-*g*-PTMC$_{32}$ network tends to become softer and
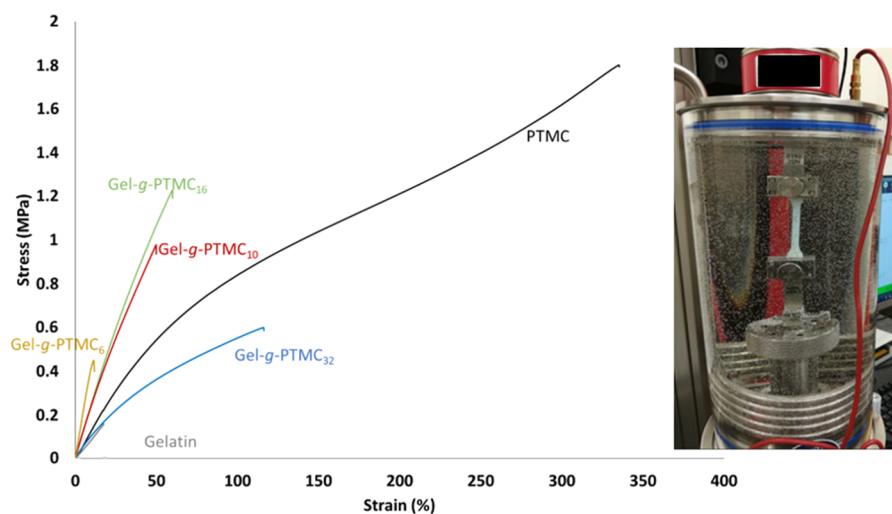
Figure 6. Mechanical properties of photocrosslinked gelatin, PTMC, and the hybrid copolymer Gel-g-PTMC$_n$ with increasing DP$_n$ values.
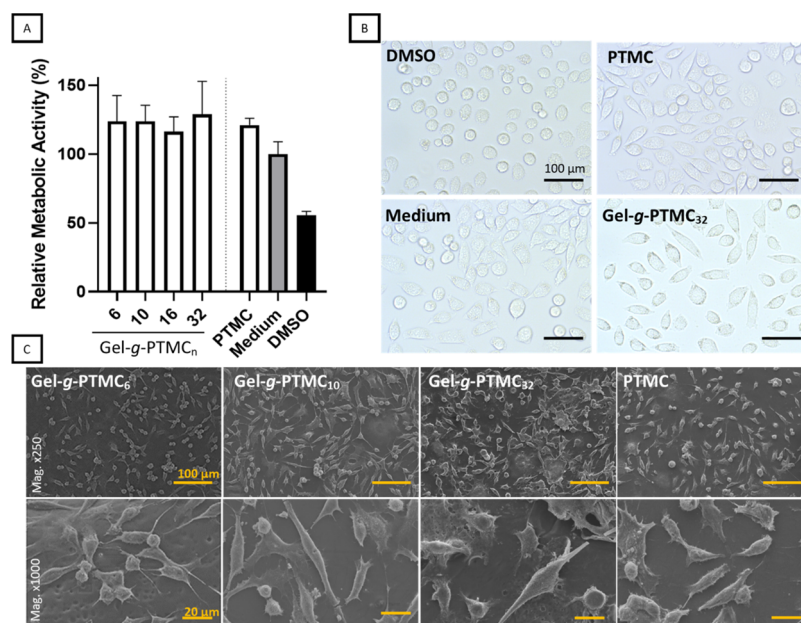
Figure 7. Indirect cytotoxicity assay: Relative metabolic activity of L929 fibroblasts cultured in sample extracts or extract-free media for 24 h. Ctrl (+) is the extract-free medium and Ctrl (−) is the culture medium supplemented with 5% DMSO. The statistical analysis, performed by one-way ANOVA with Tukey post-test, with $p < 0.01$ ($n = 6$), did not show any differences when comparing Ctrl (+) to extract media (A). The morphology of L929 fibroblasts was similar after incubation with the different extracts (B). Direct cytotoxicity assay: SEM images of the cells proliferating onto the films of Gel-g-PTMC$_n$, mag. 250 (top row) and 1000 (bottom row) (C). Photocrosslinked Gel-MA has not been included in this study due to its well-known biocompatibility property.

more elastic, with the elastic modulus falling down to 0.95 MPa and the stress at break down to 0.48 MPa. This typical evolution can be correlated with the mechanical properties of a photocrosslinked PTMC homopolymer, where low molecular weights are rather stiff with low elongation, while the elasticity increases with a higher degree of polymerization.[41] Interestingly, between Gel-g-PTMC$_{10}$ and Gel-g-PTMC$_{16}$ networks, the low evolution of the mechanical properties is visible, which means that there may exist a threshold of PTMC length where the mechanical properties are stable and others where they significantly progress. These results demonstrated the relevance of the association between gelatin and PTMC by grafting while they are both immiscible.

3.4. Cytocompatibility of the Hybrid Polymer Network Gel-g-PTMC$_n$. Gelatin and PTMC are both biocompat-

ible polymers and have been approved by Food and Drug Administration in various applications. However, the chemical modification applied to obtain photopolymerizable Gel-g-PTMC$_n$ might induce potential adverse effects on cell viability (e.g., leachable chemical substances). To detect possible leachable cytotoxic compounds, we performed an extract test according to ISO 10993-5. Figure 7A represents the relative metabolic activity of L929 fibroblasts that were cultured in the extracts of Gel-g-PTMC$_n$ with increasing amount of PTMC, normalized against medium (ctrl +). The extractions performed in the cell culture medium revealed no significant adverse effect on the viability of L929 fibroblasts up to 72 h of the culture for any of the applied materials. Ctrl (−) based on 5% DMSO showed a sign of cytotoxicity as a reduction of the metabolic activity of L929 of 45% was detected. The

morphology of the fibroblasts that were cultivated in sample extracts was similar to that of the positive control group and exhibited a spreading phenotype. Once more, cells incubated with 5% DMSO exhibited a distinct behavior, with a significantly more pronounced round-like morphology, a sign of cytotoxicity (Figure 7B).

A direct cytotoxicity assay was performed by directly seeding the fibroblasts onto the Gel-g-PTMC$_n$ films (Figure 7C). After 72 h of proliferation, all the groups allowed cells to adhere and to colonize the surface of the films, independent of their chemical composition. The morphology of the adhering cells is similar, with numerous filopodia and extensive cytoplasmic elongation. Mitotic cells are distinguished in all the groups, which supports the compatible nature of the biomaterials.

Overall, the cytocompatibility tests confirmed that the newly Gel-g-PTMC$_n$ copolymers are compatible. No significant differences were observed between the groups with various PTMC lengths, neither in adhesion nor in proliferation. Further analyses are required to assess if the presence of gelatin further strengthens the cell adhesion as we hypothesized due to the presence of RGD motif in gelatin, which is absent in PTMC.

3.5. Degradation Study of the Hybrid Polymer Network Gel-g-PTMC$_n$.
To determine the degradation mechanism, we performed a preliminary study using an accelerated degradation condition. The degradation studies were evaluated on disk samples based on photocrosslinked Gel-g-PTMC$_n$ and photocrosslinked gelatin (Figure 8). In
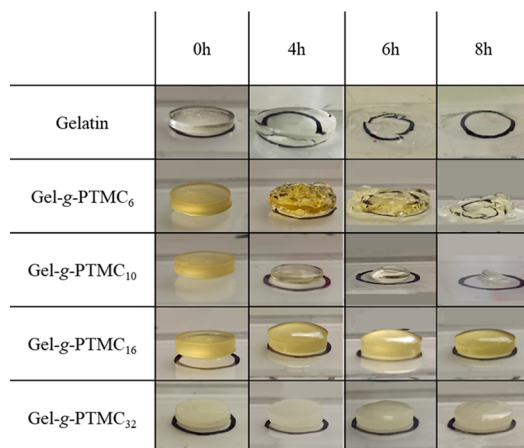
Figure 8. Pictures of the degraded Gel-g-PTMC$_n$ and gelatin networks at different incubation time points in a solution of NaOH (1 M) at 40 °C.

addition, when it was possible, the mass loss and the surface erosion were plotted (Figure S3). Interestingly, the degradation behavior of each grafted PTMC was different. Copolymers with the lowest amount of PTMC (Gel-g-PTMC$_6$) behave similarly to the photocrosslinked gelatin, which typically tend to swell after 4 h and then collapse after 6 h, which then hinder the possibility to determine properly the mass loss of the samples (Figure S3A). Such initial swelling behavior can be explained by the size of the network meshes that increases upon degradation and consequently absorbs more water. After 8 h, the gelatin is almost fully degraded, while Gel-g-PTMC$_6$ is disintegrated in several gel parts. In contrast, for the copolymer Gel-g-PTMC$_{10}$, a surface erosion behavior is noticed, which seems to help the samples maintain their physical integrity until total degradation (93% of surface erosion after 8 h) (Figure S3B). The kinetics of surface erosion is PTMC-dependent. Indeed, we observed that Gel-g-PTMC$_{16}$ degrades slowly with a slight start of erosion after 8 h, whereas Gel-g-PTMC$_{32}$ did not show any degradation in the timescale of the study. This last behavior is classically observed for crosslinked PTMC, in which the degradation mechanism relies mostly on enzymatic digestion.

3.6. Design and Scaffold Fabrication by Stereolithography.
Finally, the photoreactivity of the hybrid polymers makes it possible for the resin to be used in additive manufacturing by vat photopolymerization. The ink of Gel-g-PTMC$_n$-MA was processed in an SLA approach using a DLP apparatus. Having an appropriate resin viscosity is important to ensure efficient processability, and ideally, a resin viscosity around 1 to 10 Pa·s must be reached. Therefore, following the rheological measurement (Figure S1), the viscosities for Gel-g-PTMC$_n$ solution diluted in 20 wt % DMSO were not suitable, as they were much higher than the ideal viscosity for SLA. Consequently, all the resins were then further diluted in 40 wt % DMSO.

To demonstrate the potential of such hybrid resins to be processed in SLA, we initially designed a squared scaffold with basic cubic porosity architectures (Figure 9A). 3D porous structures were successfully built by SLA using all the Gel-g-PTMC$_n$-MA (Figure 9B). Pictures show the high performance of the fabrication in remarkable respect of the fabrication compared to the initial STL file. The layer-by-layer pattern is visible in Figure 9C, with a layer thickness of approximately 100 μm. Finally, Figure 9B shows picture scaffolds just after building (left scaffold) and after DMSO extraction and drying (right scaffold). As 40 wt % DMSO was used to reach the appropriate viscosity for fabrication by SLA, the scaffold lost 33% of its initial volume after extraction and drying. This shrinking behavior is in correlation with previous studies with
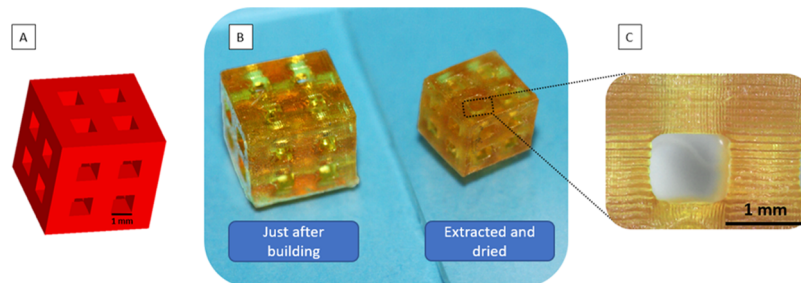
Figure 9. STL format of the designed scaffold (A), pictures of the SLA-produced 3D porous scaffold using Gel-g-PTMC$_{10}$ with different treatment conditions (B), and optical microscopy view of the scaffold (C).

PTMC resins for SLA.[6,42] One great advantage of our copolymers is the possibility to attain such a high concentration and, consequently, such a high resin viscosity, which is a prerequisite for SLA fabrication.

PTMC has great potential to be used for the TE strategy, which is highlighted by the numerous reports available in the literature.[9] One can nevertheless not forget to mention that whenever strong cell adhesion is needed, surface or bulk modification of the PTMC polymer is needed. As a first proof of concept, we show that upon methacrylation, high-resolution 3D porous scaffolds of Gel-g-PTMC$_n$ can be fabricated by SLA. Perspective works will be dedicated to further assess how the presence of gelatin moieties enhances the kinetics of cell adhesion within a scaffold.

4. CONCLUSIONS

Hybrid polymers Gel-g-PTMC$_n$ resulting from the grafting of synthetic biocompatible PTMC on natural gelatin were successfully achieved with a large range of properties regarding the length of the grafted PTMC blocks. First, the challenging characterization of covalent association between synthetic and natural polymers was unlocked by diffusion and a quantitative NMR spectroscopy approach considering the selective solubility of the precursors. Moreover, the ROP of the TMC moiety from the gelatin was obtained with high monomer conversions and remarkable high yields. Second, homogeneous photocrosslinking films based on Gel-g-PTMC$_n$ have shown promising mechanical improvement with effective cytocompatibility and cell bioadhesion, independent of the chemical composition. The degradation study allows one to decipher the key role of PTMC in Gel-g-PTMC$_n$ copolymers, with a shift from bulk to surface degradation mechanism when increasing the ratio of PTMC. Impressively, all the Gel-g-PTMC$_n$-MA in solution led to appropriate viscosity while keeping a high degree of concentration to successfully build a well-defined 3D structure with highly controlled porosity by SLA. These promising results open perspectives in the challenging field of hybrid polymer characterization and in the research of biomaterials adapted for additive manufacturing with suitable properties for tissue engineering application.

ASSOCIATED CONTENT

Ⓢ Supporting Information

The Supporting Information is available free of charge at https://pubs.acs.org/doi/10.1021/acs.biomac.1c00687.

> Viscosity of the Gel-g-PTMC$_n$ precursor resins; SEM images of Gel-g-PTMC$_n$ networks; effect of the hydrolytic degradation on mass loss and surface erosion (PDF)

AUTHOR INFORMATION

Corresponding Author

    Sébastien Blanquer − ICGM, Univ. Montpellier, CNRS, ENSCM, Montpellier 34095, France; ⓞ orcid.org/0000-0002-5366-6530; Email: sebastien.blanquer@umontpellier.fr

Authors

    Thomas Brossier − ICGM, Univ. Montpellier, CNRS, ENSCM, Montpellier 34095, France; 3D Medlab, Marignane 13700, France

    Gael Volpi − 3D Medlab, Marignane 13700, France

    Jonaz Vasquez-Villegas − LMGC, Univ. Montpellier, CNRS, Montpellier 34090, France

    Noémie Petitjean − LMGC, Univ. Montpellier, CNRS, Montpellier 34090, France; IRMB, Univ. Montpellier, INSERM, Montpellier 34090, France

    Olivier Guillaume − 3D Printing and Biofabrication Group, Institute of Materials Science and Technology, 1060 Vienna, Austria; ⓞ orcid.org/0000-0003-0735-113X

    Vincent Lapinte − ICGM, Univ. Montpellier, CNRS, ENSCM, Montpellier 34095, France

Complete contact information is available at:
https://pubs.acs.org/10.1021/acs.biomac.1c00687

Author Contributions

The manuscript was written through contributions of all authors. All authors have given approval to the final version of the manuscript.

Notes

The authors declare no competing financial interest.

■ ACKNOWLEDGMENTS

■ REFERENCES

(1) Jafari, M.; Paknejad, Z.; Rad, M. R.; Motamedian, S. R.; Eghbal, M. J.; Nadjmi, N.; Khojasteh, A. Polymeric scaffolds in tissue engineering: a literature review. *J. Biomed. Mater. Res., Part B* **2017**, *105*, 431−459.

(2) Van Vlierberghe, S.; Dubruel, P.; Schacht, E. Biopolymer-Based Hydrogels As Scaffolds for Tissue Engineering Applications: A Review. *Biomacromolecules* **2011**, *12*, 1387−1408.

(3) Guo, B. L.; Ma, P. X. Synthetic biodegradable functional polymers for tissue engineering: a brief review. *Sci. China Chem.* **2014**, *57*, 490−500.

(4) Puppi, D.; Chiellini, F. Biodegradable Polymers for Biomedical Additive Manufacturing. *Appl. Mater. Today* **2020**, *20*, 100700.

(5) Hsu, S.-h.; Hung, K.-C.; Chen, C.-W. Biodegradable polymer scaffolds. *J. Mater. Chem. B* **2016**, *4*, 7493−7505.

(6) Guillaume, O.; Geven, M. A.; Varjas, V.; Varga, P.; Gehweiler, D.; Stadelmann, V. A.; Smidt, T.; Zeiter, S.; Sprecher, C.; Bos, R. R. M.; Grijpma, D. W.; Alini, M.; Yuan, H.; Richards, G. R.; Tang, T.; Qin, L.; Yuxiao, L.; Jiang, P.; Eglin, D. Orbital floor repair using patient specific osteoinductive implant made by stereolithography. *Biomaterials* **2020**, *233*, 119721.

(7) van Bochove, B.; Hannink, G.; Buma, P.; Grijpma, D. W. Preparation of Designed Poly(trimethylene carbonate) Meniscus Implants by Stereolithography: Challenges in Stereolithography. *Macromol. Biosci.* **2016**, *16*, 1853−1863.

(8) Blanquer, S. B. G.; Gebraad, A. W. H.; Miettinen, S.; Poot, A. A.; Grijpma, D. W.; Haimi, S. P. Differentiation of adipose stem cells seeded towards annulus fibrosus cells on a designed poly(trimethylene carbonate) scaffold prepared by stereolithography. *J. Tissue Eng. Regener. Med.* **2017**, *11*, 2752−2762.

(9) Fukushima, K. Poly(trimethylene carbonate)-based polymers engineered for biodegradable functional biomaterials. *Biomater. Sci.* **2016**, *4*, 9−24.

(10) Vyner, M. C.; Li, A.; Amsden, B. G. The effect of poly(trimethylene carbonate) molecular weight on macrophage

behavior and enzyme adsorption and conformation. *Biomaterials* **2014**, *35*, 9041−9048.

(11) Asti, A.; Gioglio, L. Natural and synthetic biodegradable polymers: different scaffolds for cell expansion and tissue formation. *Int. J. Artif. Organs* **2014**, *37*, 187−205.

(12) Klimek, K.; Ginalska, G. Proteins and Peptides as Important Modifiers of the Polymer Scaffolds for Tissue Engineering Applications-A Review. *Polymer* **2020**, *12*, 844.

(13) Liu, X.; Holzwarth, J. M.; Ma, P. X. Functionalized Synthetic Biodegradable Polymer Scaffolds for Tissue Engineering. *Macromol. Biosci.* **2012**, *12*, 911−919.

(14) Ullah, S.; Chen, X. Fabrication, applications and challenges of natural biomaterials in tissue engineering. *Appl. Mater. Today* **2020**, *20*, 100656.

(15) Yi, S.; Ding, F.; Gong, L.; Gu, X. Extracellular Matrix Scaffolds for Tissue Engineering and Regenerative Medicine. *Curr. Stem Cell Res. Ther.* **2017**, *12*, 233−246.

(16) Levett, P. A.; Melchels, F. P. W.; Schrobback, K.; Hutmacher, D. W.; Malda, J.; Klein, T. J. A biomimetic extracellular matrix for cartilage tissue engineering centered on photocurable gelatin, hyaluronic acid and chondroitin sulfate. *Acta Biomater.* **2014**, *10*, 214−223.

(17) Klotz, B. J.; Gawlitta, D.; Rosenberg, A. J. W. P.; Malda, J.; Melchels, F. P. W. Gelatin-Methacryloyl Hydrogels: Towards Biofabrication-Based Tissue Repair. *Trends Biotechnol.* **2016**, *34*, 394−407.

(18) Echave, M. C.; Burgo, L. S.; Pedraz, J. L.; Orive, G. Gelatin as Biomaterial for Tissue Engineering. *Curr. Pharm. Des.* **2017**, *23*, 3567−3584.

(19) Comeau, P.; Willett, T. A Carbodiimide Coupling Approach for PEGylating GelMA and Further Tuning GelMA Composite Properties. *Macromol. Mater. Eng.* **2021**, *306*, 2000604.

(20) Kushibiki, T.; Matsuoka, H.; Tabata, Y. Synthesis and physical characterization of poly(ethylene glycol)-gelatin conjugates. *Biomacromolecules* **2004**, *5*, 202−208.

(21) Nie, K.; Han, S.; Yang, J.; Sun, Q.; Wang, X.; Li, X.; Li, Q. Enzyme-Crosslinked Electrospun Fibrous Gelatin Hydrogel for Potential Soft Tissue Engineering. *Polymer* **2020**, *12*, 1977.

(22) Hoch, E.; Hirth, T.; Tovar, G. E. M.; Borchers, K. Chemical tailoring of gelatin to adjust its chemical and physical properties for functional bioprinting. *J. Mater. Chem. B* **2013**, *1*, 5675−5685.

(23) Joy, J.; Aid-Launais, R.; Pereira, J.; Pavon-Djavid, G.; Ray, A. R.; Letourneur, D.; Meddahi-Pellé, A.; Gupta, B. Gelatin-polytrimethylene carbonate blend based electrospun tubular construct as a potential vascular biomaterial. *Mater. Sci. Eng.: C* **2020**, *106*, 110178.

(24) Liang, J.; Grijpma, D. W.; Poot, A. A. Tough and biocompatible hybrid networks prepared from methacrylated poly(trimethylene carbonate) (PTMC) and methacrylated gelatin. *Eur. Polym. J.* **2020**, *123*, 109420.

(25) Dai, M.; Goudounet, G.; Zhao, H.; Garbay, B.; Garanger, E.; Pecastaings, G.; Schultze, X.; Lecommandoux, S. Thermosensitive Hybrid Elastin-like Polypeptide-Based ABC Triblock Hydrogel. *Macromolecules* **2021**, *54*, 327−340.

(26) Zhang, Y.; Wu, K.; Sun, H.; Zhang, J.; Yuan, J.; Zhong, Z. Hyaluronic Acid-Shelled Disulfide-Cross-Linked Nanopolymersomes for Ultrahigh-Efficiency Reactive Encapsulation and CD44-Targeted Delivery of Mertansine Toxin. *ACS Appl. Mater. Interfaces* **2018**, *10*, 1597−1604.

(27) Chartrain, N. A.; Williams, C. B.; Whittington, A. R. A review on fabricating tissue scaffolds using vat photopolymerization. *Acta Biomater.* **2018**, *74*, 90−111.

(28) Shirahama, H.; Lee, B. H.; Tan, L. P.; Cho, N.-J. Precise Tuning of Facile One-Pot Gelatin Methacryloyl (GelMA) Synthesis. *Sci. Rep.* **2016**, *6*, 31036.

(29) Kale, R. N.; Bajaj, A. N. Ultraviolet Spectrophotometric Method for Determination of Gelatin Crosslinking in the Presence of Amino Groups. *J. Young Pharm.* **2010**, *2*, 90−94.

(30) Brossier, T.; Volpi, G.; Lapinte, V.; Blanquer, S. Synthesis of Poly(Trimethylene Carbonate) from Amine Group Initiation: Role of Urethane Bonds in the Crystallinity. *Polymer* **2021**, *13*, 280.

(31) Claassen, C.; Claassen, M. H.; Truffault, V.; Sewald, L.; Tovar, G. E. M.; Borchers, K.; Southan, A. Quantification of Substitution of Gelatin Methacryloyl: Best Practice and Current Pitfalls. *Biomacromolecules* **2018**, *19*, 42−52.

(32) Ovsianikov, A.; Deiwick, A.; Van Vlierberghe, S.; Dubruel, P.; Möller, L.; Dräger, G.; Chichkov, B. Laser Fabrication of Three-Dimensional CAD Scaffolds from Photosensitive Gelatin for Applications in Tissue Engineering. *Biomacromolecules* **2011**, *12*, 851−858.

(33) Stevens, P. V. Trace Bioorganic Constituents of Gelatins - a Review. *Food Aust.* **1992**, *44*, 320−324.

(34) Yue, K.; Li, X.; Schrobback, K.; Sheikhi, A.; Annabi, N.; Leijten, J.; Zhang, W.; Zhang, Y. S.; Hutmacher, D. W.; Klein, T. J.; Khademhosseini, A. Structural analysis of photocrosslinkable methacryloyl-modified protein derivatives. *Biomaterials* **2017**, *139*, 163−171.

(35) Toshikj, N.; Robin, J.-J.; Blanquer, S. A simple and general approach for the synthesis of biodegradable triblock copolymers by organocatalytic ROP from poly(lactide) macroinitiators. *Eur. Polym. J.* **2020**, *127*, 109599.

(36) Li, X.; Mignard, N.; Taha, M.; Fernández-de-Alba, C.; Chen, J.; Zhang, S.; Fort, L.; Becquart, F. Synthesis of Poly(trimethylene carbonate) Oligomers by Ring-Opening Polymerization in Bulk. *Macromol. Chem. Phys.* **2020**, *221*, 1900367.

(37) Alba, A.; du Boullay, O. T.; Martin-Vaca, B.; Bourissou, D. Direct ring-opening of lactide with amines: application to the organo-catalyzed preparation of amide end-capped PLA and to the removal of residual lactide from PLA samples. *Polym. Chem.* **2015**, *6*, 989−997.

(38) Anastasio, R.; Peerbooms, W.; Cardinaels, R.; van Breemen, L. C. A. Characterization of Ultraviolet-Cured Methacrylate Networks: From Photopolymerization to Ultimate Mechanical Properties. *Macromolecules* **2019**, *52*, 9220−9231.

(39) Shin, H.; Olsen, B. D.; Khademhosseini, A. The mechanical properties and cytotoxicity of cell-laden double-network hydrogels based on photocrosslinkable gelatin and gellan gum biomacromolecules. *Biomaterials* **2012**, *33*, 3143−3152.

(40) Pêgo, A. P.; Grijpma, D. W.; Feijen, J. Enhanced mechanical properties of 1,3-trimethylene carbonate polymers and networks. *Polymer* **2003**, *44*, 6495−6504.

(41) Schüller-Ravoo, S.; Feijen, J.; Grijpma, D. W. Flexible, elastic and tear-resistant networks prepared by photo-crosslinking poly-(trimethylene carbonate) macromers. *Acta Biomater.* **2012**, *8*, 3576−3585.

(42) Blanquer, S. B. G.; Werner, M.; Hannula, M.; Sharifi, S.; Lajoinie, G. P. R.; Eglin, D.; Hyttinen, J.; Poot, A. A.; Grijpma, D. W. Surface curvature in triply-periodic minimal surface architectures as a distinct design parameter in preparing advanced tissue engineering scaffolds. *Biofabrication* **2017**, *9*, No. 025001.